# Characterization of Sulfonated Polysulfone Membranes Modified by Ion Beam Irradiation

*Rama Chennamsetty, Isabel Escobar*
*Department of Chemical & Environmental engineering, The University of Toledo,*
*2801 West Bancroft, Nitschke Hall 3048, Toledo, OH 43606, United States*
*Tel: +419 530 6079, Fax 419 530 8086, E-mail: chennamsetty@gmail.com*

## Abstract

Ion Beam irradiation was used to modify the surface of a sulfonated polysulfone water treatment membrane. A beam of 25 keV $H^+$ ions with three irradiation fluences ($1\times10^{13}$ ions/cm$^2$, $5\times10^{13}$ ions/cm$^2$, and $1\times10^{14}$ ions/cm$^2$) was used for membrane irradiation. ATR-FTIR analyses were performed on the virgin and irradiated membranes in order to determine the changes to chemical structure incurred by ion beam irradiation. The results show that some of the sulphonic and C-H bonds were broken and new C-S bonds were formed after irradiation. AFM analyses show that membrane roughness decreased after irradiation. A significant increase in flux after ion beam irradiation was also observed, while the amount of cake accumulation on the membrane was decreased after ion beam irradiation. Hyhrophobicity, pore size distribution and selectivity of the membrane were not affected by ion beam irradiation.

*Key words:* Ion Beam Radiation, Surface Modifications, Membrane, Ion Fluence

## Introduction

Membranes are becoming a common means of separation in the water treatment field because they can be designed to meet stringent standards while requiring significantly less space and time than other separation techniques. Ideal membranes would be able to maintain high throughput of a desired permeate with a high degree of selectivity. Unfortunately, these two parameters are mutually counteractive. The reason is that a high degree of selectivity is normally only achievable using a membrane having small pores and inherently high hydraulic resistance (or low permeability). Fouling is another severe problem associated with water treatment membranes, which is the deposition of solute constituents onto the surface of the membrane. Fouling of membrane elements often causes a significant increase in hydraulic resistance and applied pressure drop, which increases operating cost and decreases the life of the membrane [1].

For membranes to be competitive with conventional technologies, a membrane process needs to operate with a high rate of flux, have a high degree of selectivity and have a high resistance to fouling. There are three main areas of interest when it comes to improving membrane performance: the synthesis process, the application process, and post-synthesis modification. Synthesis process improvement involves the techniques, methods and materials of the manufacturing processes to produce a high performance membrane. The application process involves the specific operating parameters for a membrane system. These include selecting the raw water characteristics, operating pressure and cleaning intervals to allow the system to operate at maximum efficiency. Post-synthesis modification involves modifying the

membrane after the initial manufacturing process is complete, which was the focus of the study discussed here.

One such post synthesis modification is achieved through ion beam irradiation. Ion beam irradiation has long been recognized as an effective method for the synthesis and modification of diverse materials, including polymers [2-4]. Ion beam irradiation is the bombardment of a substance with energetic ions. When the ions penetrate through the surface of a membrane, they may eliminate the tall peaks and deep valleys, resulting in an overall reduction in surface roughness [5]. As the ions penetrate the membrane, they lose energy to their surroundings (membrane structure) by two main processes: interacting with target nuclei (nuclear stopping) and interacting with target electrons (electronic stopping; [6]). Nuclear stopping energy losses arise from collisions between energetic particles and target nuclei. Atomic displacement occurs when the colliding ion imparts energy greater than certain displacement threshold energy. If the energy is not great enough for displacement, the energy dissipates as atomic vibrations known as phonons. Electronic stopping energy losses arise from electromagnetic interaction between the positively charged ions and the target electrons. Excitation and ionization are two common forms of electronic energy loss. Excitation is the process in which an electron jumps to a higher energy level, while in ionization; an orbital electron is ejected from the atom.

There have been a number of studies examining the effects of ion beam irradiation on gas separation membranes [5, 7-9]. These studies exposed polyimide gas separation membranes to different ion irradiation fluences and energies. Ion irradiation fluences refer to the number of ions implanted into a unit of area of the membrane. Ion energy quantifies the energy level of the ions, which is directly related to the depth the ions will penetrate into the membrane. As discussed earlier, ion beam irradiation provides energy to the electrons and nuclei of the membrane. The intensive energy deposition in polymers can lead to the following: (1) formation of volatile molecules and free radicals which leave defects in the polymer matrix, (2) creation of additional crosslinking between polymer chains, (3) formation of new chemical bonds, and (4) chemical reactions with chemical atmosphere such as oxidation [8]. These four events can, in turn, lead to membrane microstructure alterations. Previous studies [7-9] found ion beam irradiation resulted in gas separation membranes with both increased permeability and selectivity; two characteristics which have a trade-off relationship toward each other. The improvements in membrane performance were believed to be results of microstructure modification, which was proven by a narrow but intensive free volume distribution. Studies of atomic force microscopy (AFM) of ion beam irradiated polyimide films showed that ion beam irradiation eliminates deep valleys and tall peaks on the surface of the polyimide films even at very low doses of irradiation and that a very smooth surface can be observed after ion beam irradiation [4].

The goal of the study described here was to determine the effects of ion beam irradiation on surface morphology, microstructure, and chemical structure and on the performance of a modified commercial sulfonated polysulfone water treatment membrane.

## Experimental

### *Membrane Properties*

A commercially available nanofiltration composite membrane with a selective layer of sulfonated polysulfone was used for testing. The structure of the sulfonated polysulfone is

shown in fig.1. The membrane is negatively charged (at pH = 7.0, the charge is -6.26 mV), hydrophobic (contact angle of 58°; [10]) and has a molecular weight cutoff (MWCO) of 500 Da. The operating temperature range is 0-45°C and pH range is 2-11, and the membrane is able to withstand chlorine concentrations of several hundred ppm.

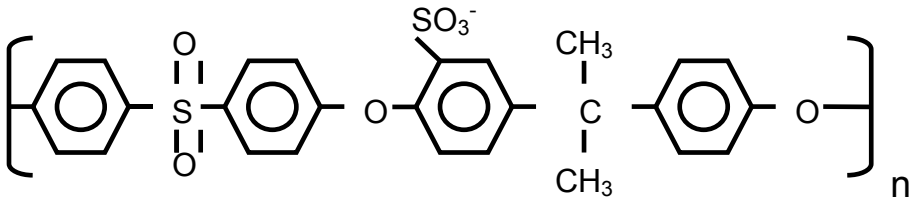


**Figure 1: Structure of Sulfonated Polysulfone**

*Ion Beam Irradiation*

Each membrane was irradiated with $H^+$ ions at an energy level of 25 keV. The incident energy of 25 keV was determined using a well-known program titled "The Stopping Range of Ion in Matter" (SRIM; [11]) to ensure that the entire upper semipermeable sulfonated polysulfone layer was modified. The thickness of the upper layer was obtained from the SEM images shown in Fig. 2, which show the cross section of the membrane. SEM images were obtained using a JSM 6100 SEM (JEOL Inc., Peabody, MA). The SEM images show that the composite membrane was characterized by a thin semipermeable sulfonated polysulfone

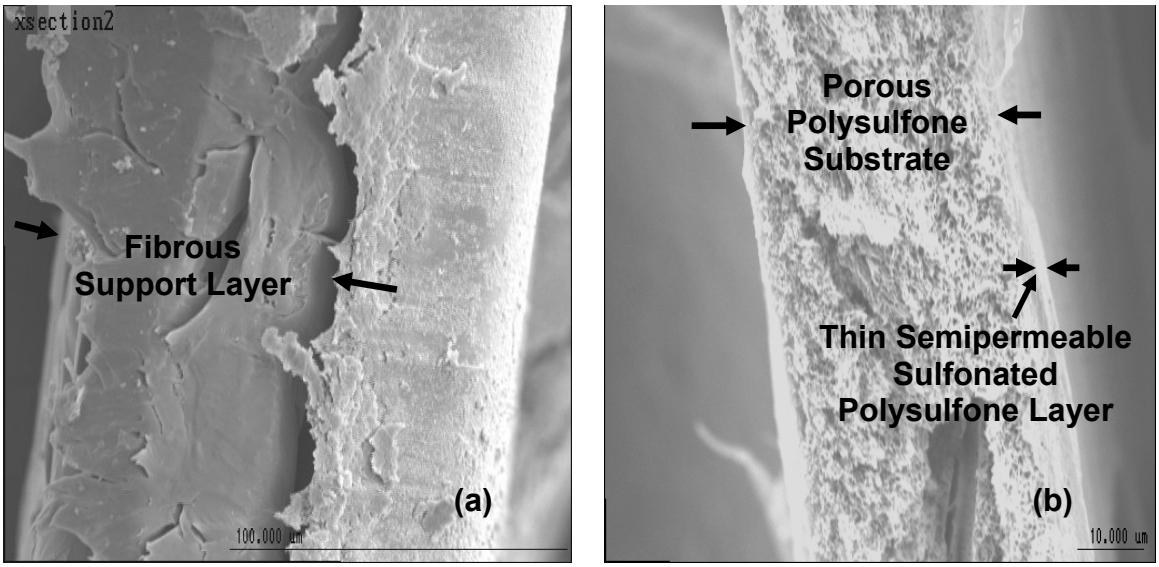


**Figure 2: SEM images of the crosssection of the membrane. (a) The three layers of the membrane (b) The top two layers of the membrane after the fibrous support layer is separated.**

membrane layer (0.2 μm thick), supported on a porous polysulfone substrate (about 50 μm thick) that, in turn, is bounded to a fibrous layer, which provides mechanical strength to the top layers without adding significant hydrodynamic resistance. The incident energy of 25 keV is chosen to ensure that the entire upper layer of approximately 0.2 μm thick is modified by the ion beam irradiation. Three irradiation fluences ($1\times10^{13}$ ions/cm$^2$, $5\times10^{13}$ ions/cm$^2$, and $1\times10^{14}$ ions/cm$^2$) were used for ion beam irradiation of the membranes. The beam current density was maintained at low levels (<1 μA/cm$^2$) to avoid heating of the samples. All samples were

irradiated at room temperature and in a vacuum chamber at a pressure less then $1.9 \times 10^{-7}$ torr. The incident beam was perpendicular to the samples. The irradiation was performed using a 1.7 MV high current Tandetron Accelerator at the University of Michigan (Ann Arbor, Michigan, USA). To provide support to the membrane through the irradiation process, a foil tape masking was utilized. Only the active area of the membrane, which was about a circular area of 95 $cm^2$, was irradiated.

*Fourier Transform Infrared Spectroscopy (FTIR) analysis*

Attenuated total reflectance fourier transform infrared spectroscopy (ATR-FTIR) was used to study the evolution of chemical structures of the nanofiltration membranes after irradiation with $H^+$ ion beam. FTIR uses measurements of vibrational spectra to identify the chemical structure of materials. FTIR measurements were performed using a Digilab UMA 600 FT-IT microscope with a Pike HATR adapter and an Excalibur FTS 400 spectrometer (Randolph, MA). The FTIR analysis on the virgin and irradiated membranes with different fluences were performed at the same condition before and after ion irradiation to monitor any changes of the spectrum induced by irradiation.

*Contact Angle Analysis*

The contact angle measurements were performed using distilled water on the top surface of the membranes using Cam-Plus Micro contact angle meter (Tantec Inc., Schaumburg, IL). Sessile Drop, Half-Angle™ measuring method (U.S. Patent No. 5,268,733) was used for measuring the contact angles. The measurements were performed at room temperature.

*Pore Size Distribution Analysis*

The pore size distribution analyses were performed using polyethylene glycol (PEG) of various molecular weights (ranging from 200 g/mol to 4600 g/mol). The sizes of the PEG molecules were obtained using Einstein-Stokes diameter [12], $a_d$, which is related to molecular weight as follows:

$$a_d \text{ (nm)} = 33.46 \times 10^{-2} M^{0.557} \qquad (1)$$

where $a_d$ is the Einstein-Stokes diameter in nm and M is the molecular weight in g/mol.

*Atomic Force Microscopy (AFM) Analysis*

Atomic force microscopy (AFM) was used for evolution in surface morphology. AFM allows acquiring 3D topographic data with a high vertical resolution. Accurate and quantitative data about surface morphology are provided over a wide range of magnifications and can be used in several quantitative analyses approaches such as section, bearing and roughness analysis. AFM measurements were performed using a Nanoscope IIIa Scanning Probe Microscopy (Digital Instruments, Santa Barbara, CA).

*Bench-Scale Cross-Flow*

The membrane was housed in a SEPA CF cross-flow filtration unit (Osmonics, Minneatonka, MN). The filtration unit was constructed out of 316 stainless steel and rated for an operating pressure up to 69 bar (1000 psi). The test unit was sealed by applying adequate pressure via a hand pump (P-142, Enerpac, Milwaukee, WI) which actuated a piston on the SEPA CF, sealing the membrane within the membrane cell. The feed stream was delivered by

a motor (Baldor Electric Company, Ft. Smith, AR and Dayton Electric Manufacturing Co., Niles, IL) and M-03 Hydracell pump (Wanner Engineering, Inc., Minneapolis, MN) assembly. Flow valves controlled permeate and retenate (also called concentrate) flow and the pressure acting on the membrane in the test unit. Due to the high pressures required by the membranes, it was necessary to control the temperature of the feed water using a chiller (Model KR60A, Cole-Parmer Instrument Company, Veenon Hills, Illinois) to keep it at approximately 20$^{o}$C. The schematic diagram of the filtration assembly is shown in figure 3.

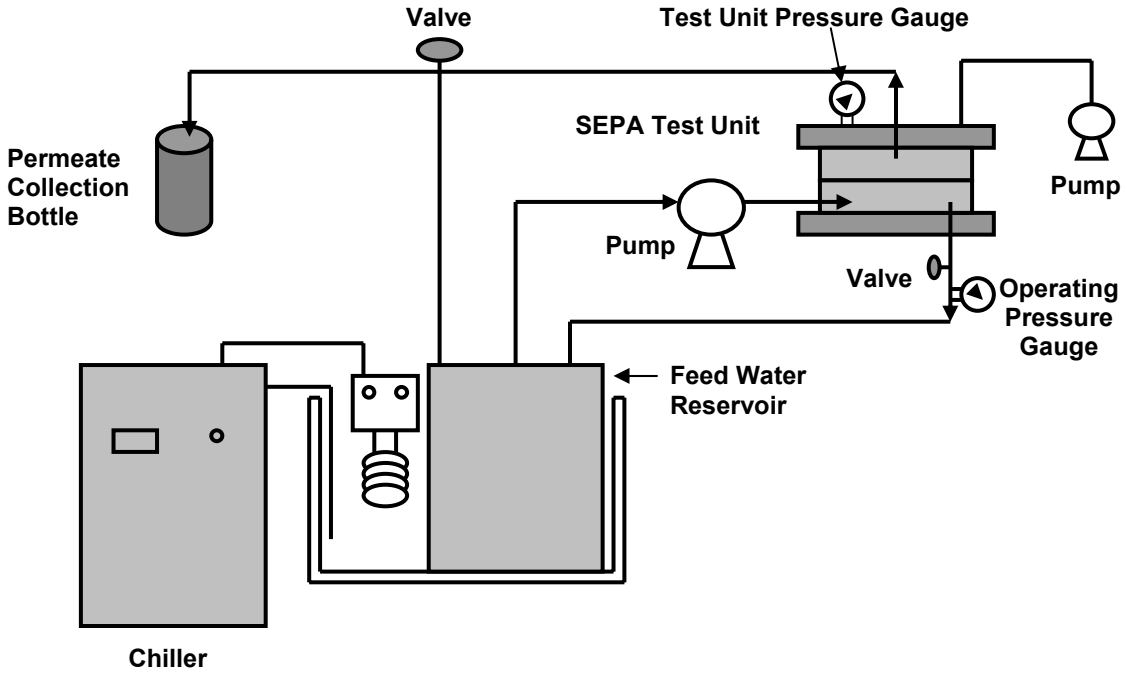


**Figure 3: Schematic Diagram Showing the Filtration Assembly**

The SEPA CF unit required a membrane area of 139 cm$^2$, but membrane size was restricted to a circular area of 95 cm$^2$ because of limitations of the chosen irradiation method. The required area was reduced to accommodate the sample size by applying a foil tape masking around the membrane (necessary also for irradiation purposes).

The membranes were tested with raw water consisting of bovine serum albumin protein with a concentration of 10 mg/L and 1 mM of $CaCl_2$. Before testing began, each membrane was thoroughly rinsed with deionized (DI) water and soaked in DI water overnight [13]. The membrane was removed from the DI water and thoroughly rinsed with DI water again immediately before placing the membrane into the filtration cell unit. After installation, the membrane was pre-compacted by filtering 250 mL of DI water [13]. The pre-soaking and initial DI water flush were required to stabilize the flux and rejection of the membrane. Initially, membrane pores were filled with air; soaking and pre-compaction forces out these air bubbles, allowing a “steady-state” operation of the membrane prior to filtration of raw water. The synthetic raw water was added to the feed reservoir and permeate samples were collected at regular intervals of time. Water quality analysis was performed by measuring the total dissolved organic carbon (DOC, Phoenix 8000, Tekmar-Dohrmann, Cincinnati, OH). After each experimental run, the membranes were taken out of the filtration cell, dried and had their surface chemistry and morphology analyzed.

## Results and Discussion

The sulfonted polysulfone membranes were bombarded at ion fluences in the following ranges: (1) small fluence at $1\times10^{13}$ $H^+$ ions/cm$^2$, (2) intermediate fluence at $5\times10^{13}$ $H^+$ ions/cm$^2$, and (3) high fluence at $1\times10^{14}$ $H^+$ ions/cm$^2$. The color of the virgin membrane was white and was changed to a light brown color after ion beam irradiation with an ion fluence of $1\times10^{13}$ $H^+$ ions/cm$^2$. The intensity of the color increased as the irradiation dose was increased from ion fluence $1\times10^{13}$ $H^+$ ions/cm$^2$ to $1\times10^{14}$ $H^+$ ions/cm$^2$.

In order to determine the effects of ion beam irradiation on the chemical structure of the membrane, ATR/FTIR analysis was performed on the irradiated membranes and was compared with the ATR/FTIR analysis of the virgin membrane. Fig.4 compares the FTIR spectra of the virgin and irradiated membranes, which shows changes in the peak heights at 690 cm$^{-1}$, 920 cm$^{-1}$ and 1041 cm$^{-1}$ wavenumbers. The peak height at 690 cm$^{-1}$ wavenumber

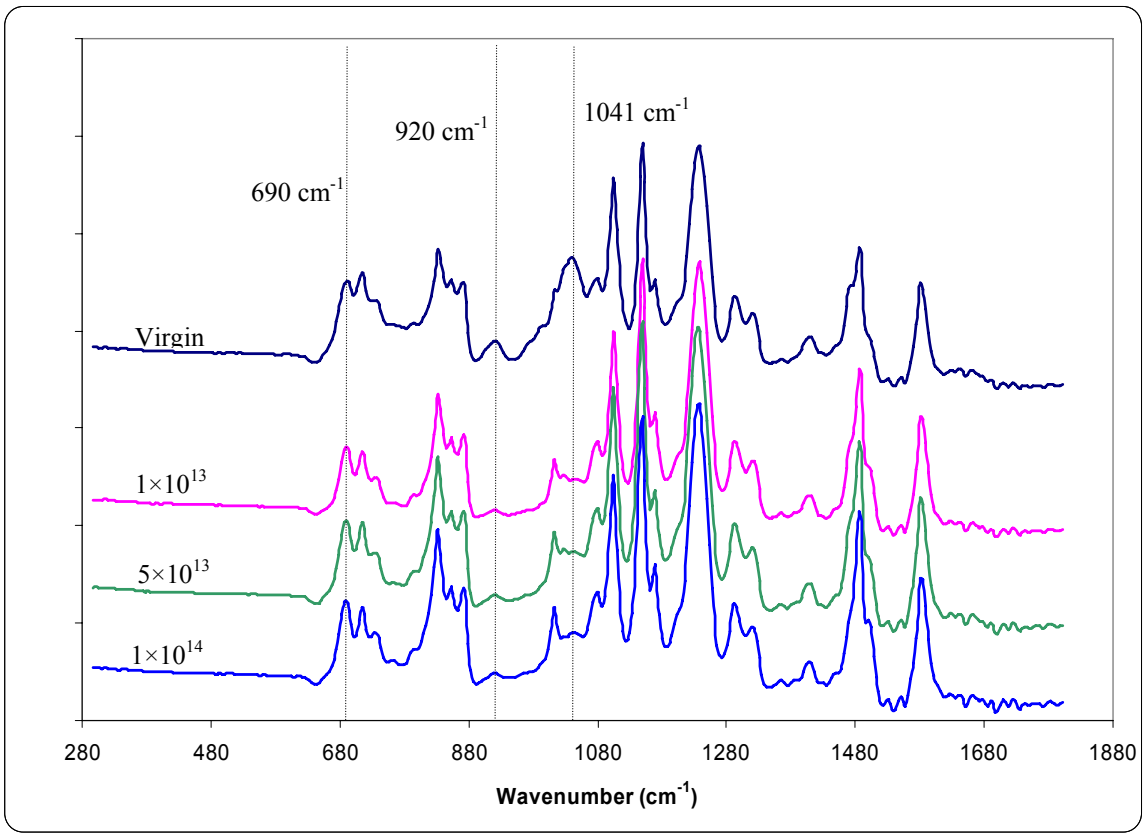


**Figure 4: Atr/Ftir Spectra for the Virgin and irradiated membranes with ion fluences of $1\times10^{13}$ ions/cm$^2$, $5\times10^{13}$ ions/cm$^2$, and $1\times10^{14}$ ions/cm$^2$**

was increased after irradiation and the peak heights at 920 cm$^{-1}$ and 1041 cm$^{-1}$ wavenumbers were decreased after irradiation. The peak at 690 cm$^{-1}$ wavenumber corresponds to the presence of C-S-C bond [14]. The peak height at this wavenumber increased with increasing ion fluence. The increase in peak height at 690 cm$^{-1}$ wavenumber as a function of ion fluence is shown in fig.5. The peak height at 920 cm$^{-1}$ wavenumber corresponds to the C-H bond out of plane vibrations [14]. The peak height at this decreased with increasing ion fluence. The decrease in peak height at 920 cm$^{-1}$ wavenumber as a function of ion fluence is shown in fig.6. The peak at 1041 cm$^{-1}$ wavenumber corresponds to the presence of $SO_3$ bond [14]. The peak height at this decreased with increasing ion fluence. The decrease in peak height at 1041 cm$^{-1}$

wavenumber as a function of ion fluence is shown in fig.7. Based on fig 4, ion beam irradiation leads to the breaking of $SO_3$ and C-H bonds along with the formation of C-S-C bonds. These are hypothesized to have led to an increase in cross linking.

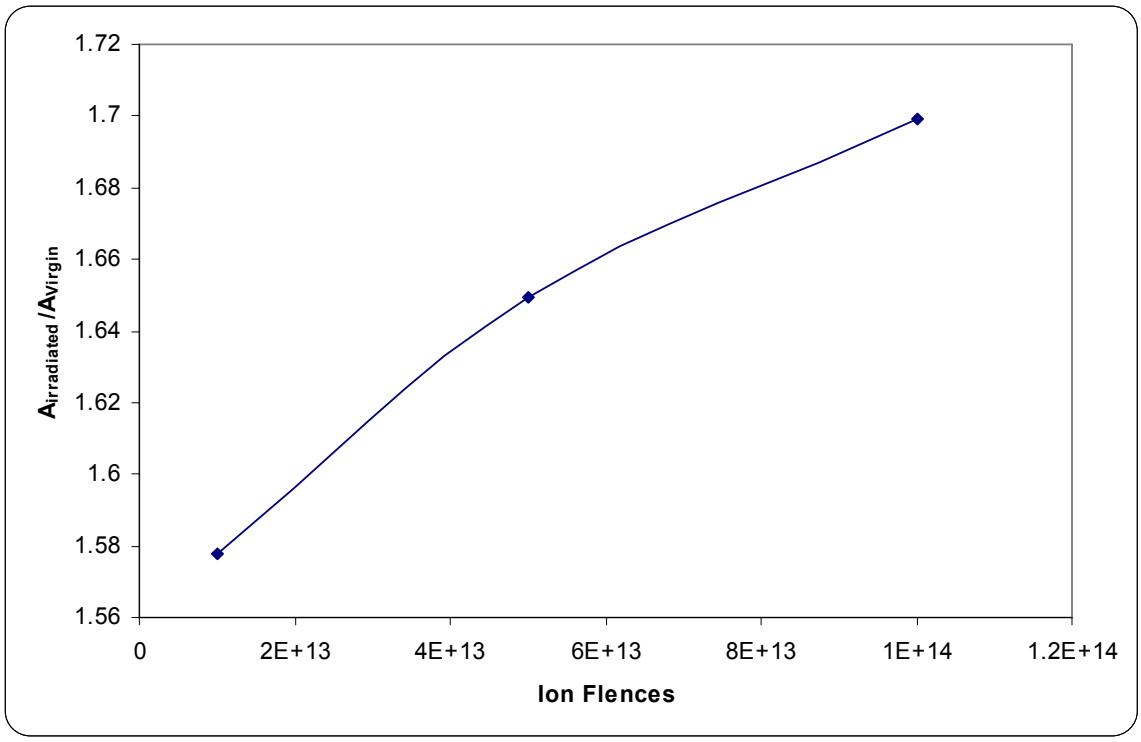


**Figure 5: Increase in absorbance at 690 $cm^{-1}$ wavenumber as a function of ion fluences**

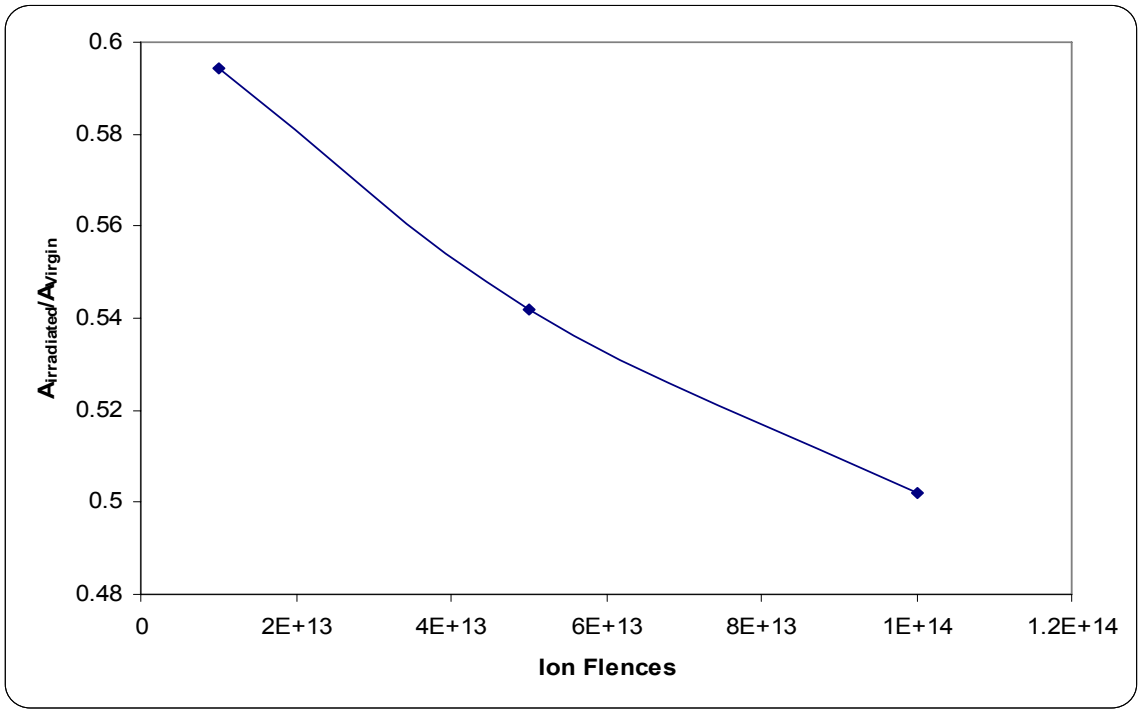


**Figure 6: Decrease in absorbance at 920 $cm^{-1}$ wavenumber as a function of ion fluences**

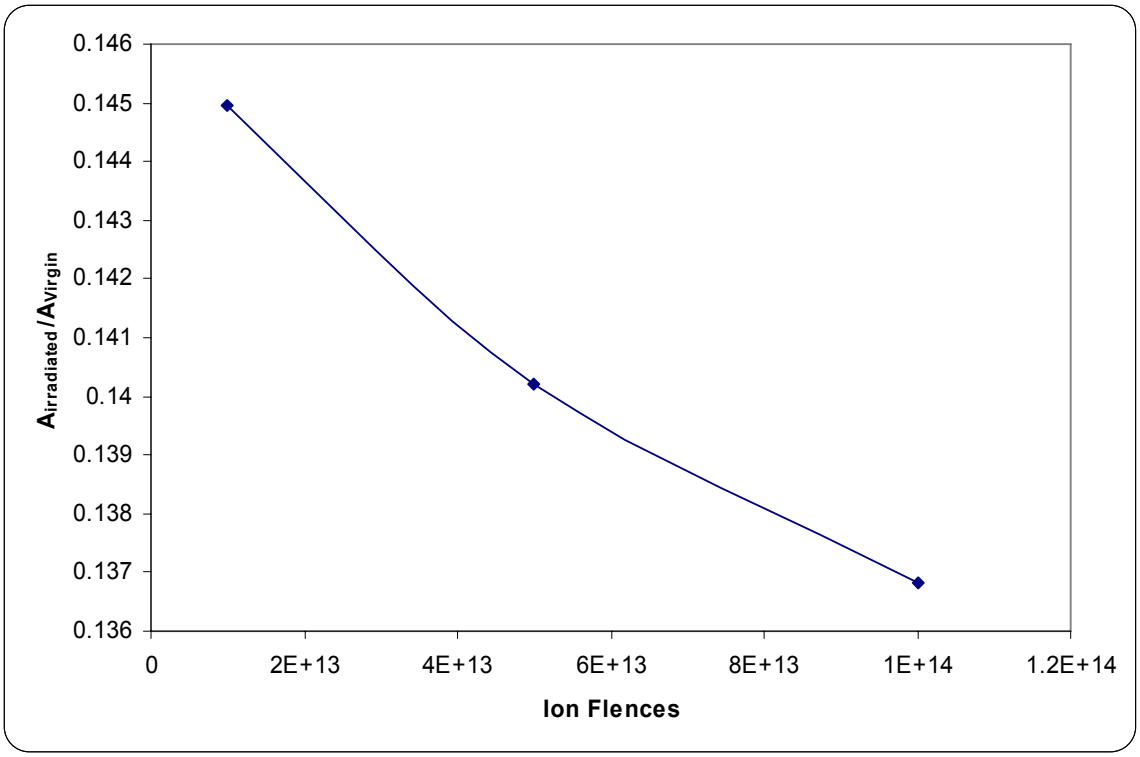


**Figure 7: Decrease in absorbance at 1041 $cm^{-1}$ wavenumber as a function of ion fluences**

The observed contact angle for the virgin membrane was approximately 59.11° (tab.1) which was consistent with values reported in the literature [10]. Tab.1 also shows that the irradiated membrane contact angles were not different from the virgin membrane, which confirmed that the hydrophobic character of the membrane was not changed after ion beam irradiation.

| Membrane Type | Contact angle |
|---|---|
| **Virgin** | 59.11° (± 6.19°) |
| **$1\times10^{13}$ Ions/$cm^2$** | 57.89° (± 2.42°) |
| **$5\times10^{13}$ Ions/$cm^2$** | 59.56° (± 2.40°) |
| **$1\times10^{14}$ Ions/$cm^2$** | 58.78° (± 2.82°) |

**Table 1: Contact angle measurements of virgin and irradiated membranes**

Fig.8 shows the AFM images of the virgin and irradiated membranes. The area of the image is 5 × 5 μm in the x, y-plane with an expanded z-axis of 5 nm. The average roughness of the virgin sulfonated polysulfone membrane was 5.63 nm (±1.32 nm) and was decreased to 3.33 nm (±0.73 nm) after irradiation of the membrane with an ion fluence of $1\times10^{13}$ ions/$cm^2$. The roughness of the irradiated membranes with ion fluences of $5\times10^{13}$ ions/$cm^2$ and $1\times10^{14}$ ions/$cm^2$ were 2.95 nm (±0.89 nm) and 2.67 nm (±0.63 nm), respectively. The average decreases in roughness were 41%, 48%, and 53% after irradiation with ion fluences of $1\times10^{13}$ ions/$cm^2$, $5\times10^{13}$ ions/$cm^2$, and $1\times10^{14}$ ions/$cm^2$, respectively, from the virgin membrane. The trend of decrease in roughness with ion fluence is shown in fig.9. AFM analyses indicate that

nodule-like structures of the unmodified membrane were smoothened after ion beam irradiation. This decrease was expected as observed with gas separation membranes [5].

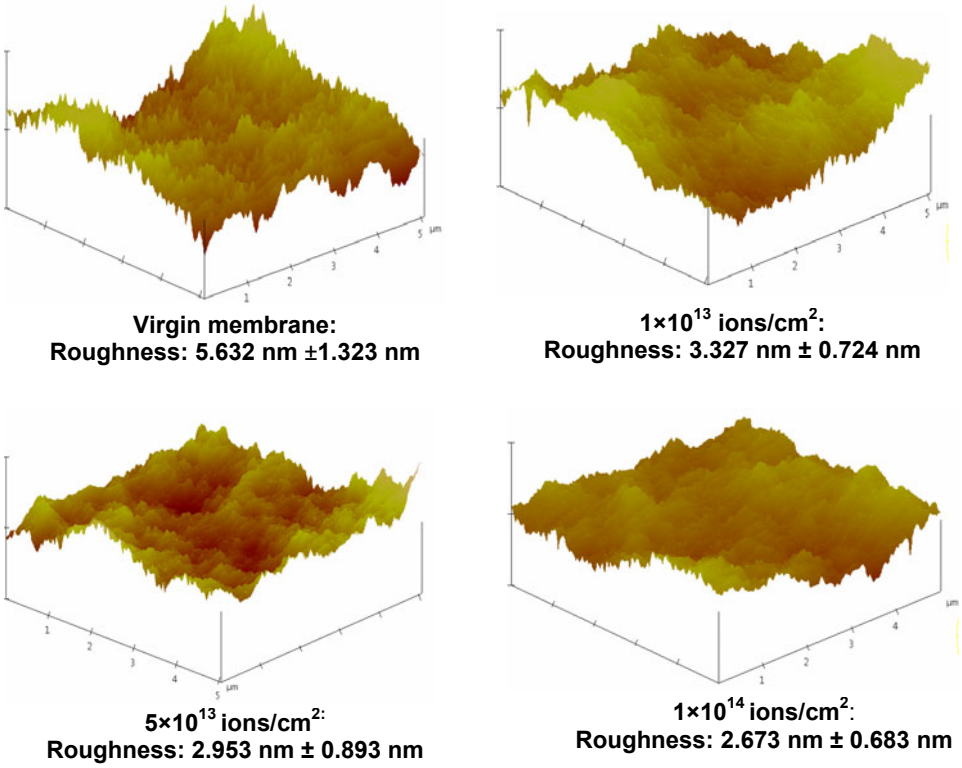

**Virgin membrane:**
**Roughness: 5.632 nm ±1.323 nm**

**$1\times10^{13}$ ions/cm$^2$:**
**Roughness: 3.327 nm ± 0.724 nm**

**$5\times10^{13}$ ions/cm$^2$:**
**Roughness: 2.953 nm ± 0.893 nm**

**$1\times10^{14}$ ions/cm$^2$:**
**Roughness: 2.673 nm ± 0.683 nm**

**Figure 8: AFM images of the membranes**

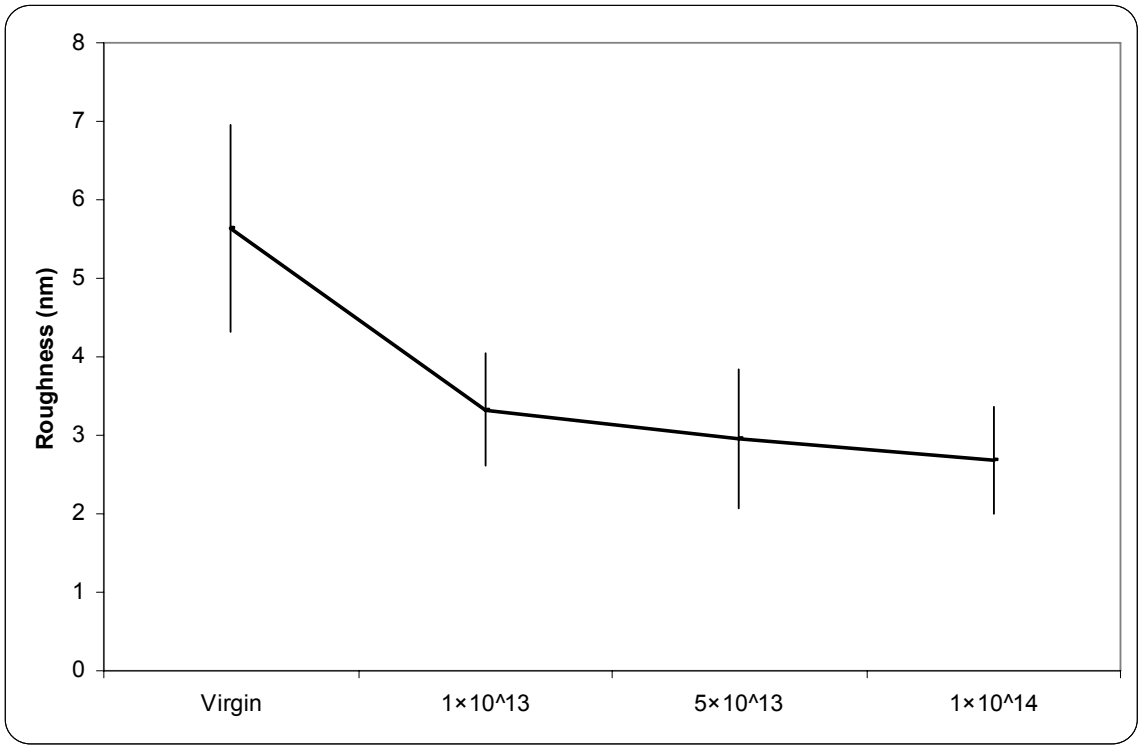


**Figure 9: Roughness of the virgin and the irradiated membranes**

Fig.10 represents the pore size distribution analyses of the virgin and irradiated membranes which show the changes in the solute rejections of model compounds with varying diameters. The analyses show that the pore size distribution was not affected by the ion beam irradiation. Since the hydrophobic character and pore size distribution were not changed after ion beam radiation, the rejection values should not change after ion beam irradiation which was confirmed by comparing the rejection values of both virgin and irradiated membranes. Fig.11 shows rejection values of the virgin and irradiated membranes when the feed water was composed of the protein and $CaCl_2$. Protein rejection values were not changed after ion beam irradiation. This also indicates that the separation capabilities of the membrane were not affected by ion beam irradiation.

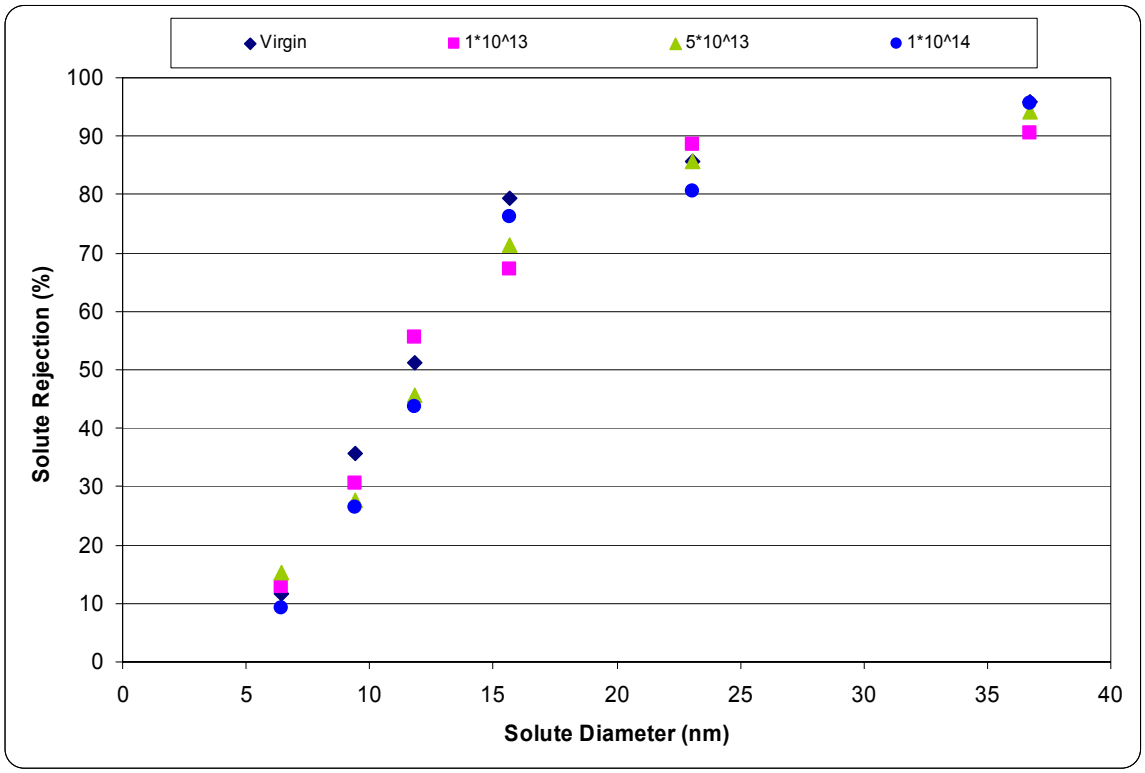


**Figure 10: Pore size distribution analysis of virgin and irradiated membranes**

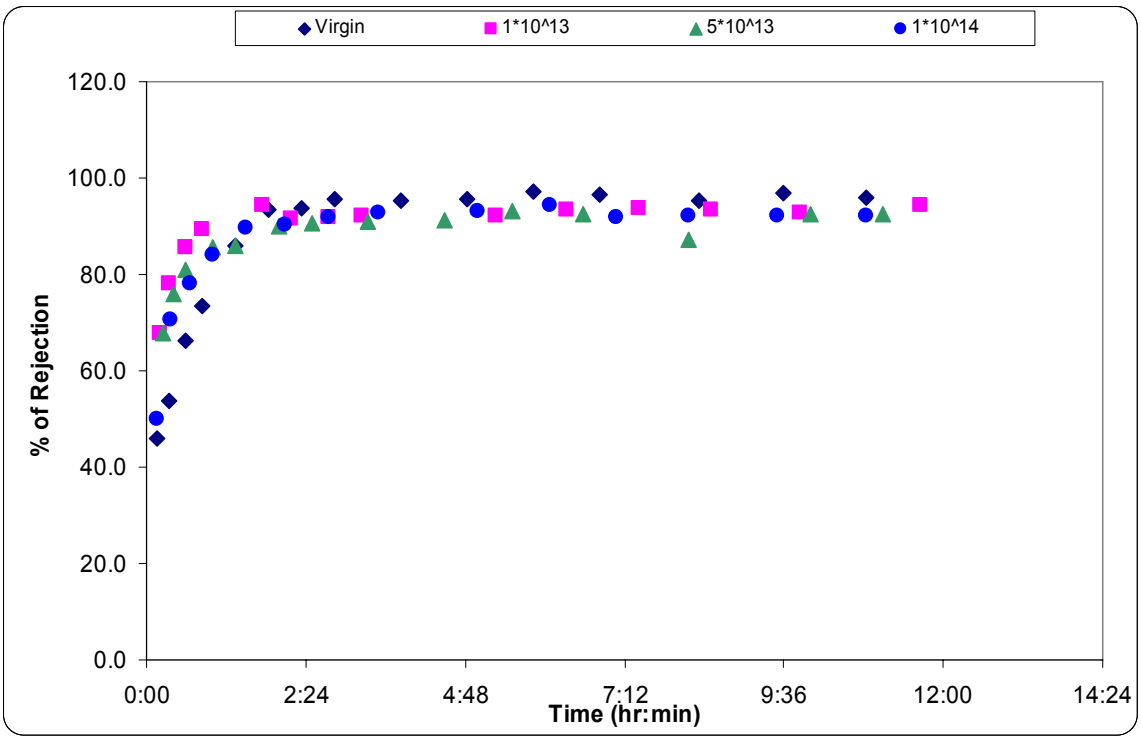


**Figure 11: Rejection Vs time of virgin and irradiated membranes**

Fig.12 represents the flux analyses for the virgin and irradiated membranes which were run with feed water containing protein and $CaCl_2$. The analyses show that the flux was increased after ion beam irradiation. The increase in the flux values for the three irradiated membranes with ion fluences $1\times10^{13}$ ions/cm$^2$, $5\times10^{13}$ ions/cm$^2$, and $1\times10^{14}$ ions/cm$^2$ were 36%, 39% and 41%, respectively, after 10 hrs of operation. Flux and selectivity have an indirect relationship; a membrane with high flux will have low selectivity, and vice versa. Fig 13 represents the relationship between flux and selectivity. Ion beam irradiation has resulted in an increase in flux without changing the selectivity of the membrane; therefore the characteristic increase relationship was improved fig.13.

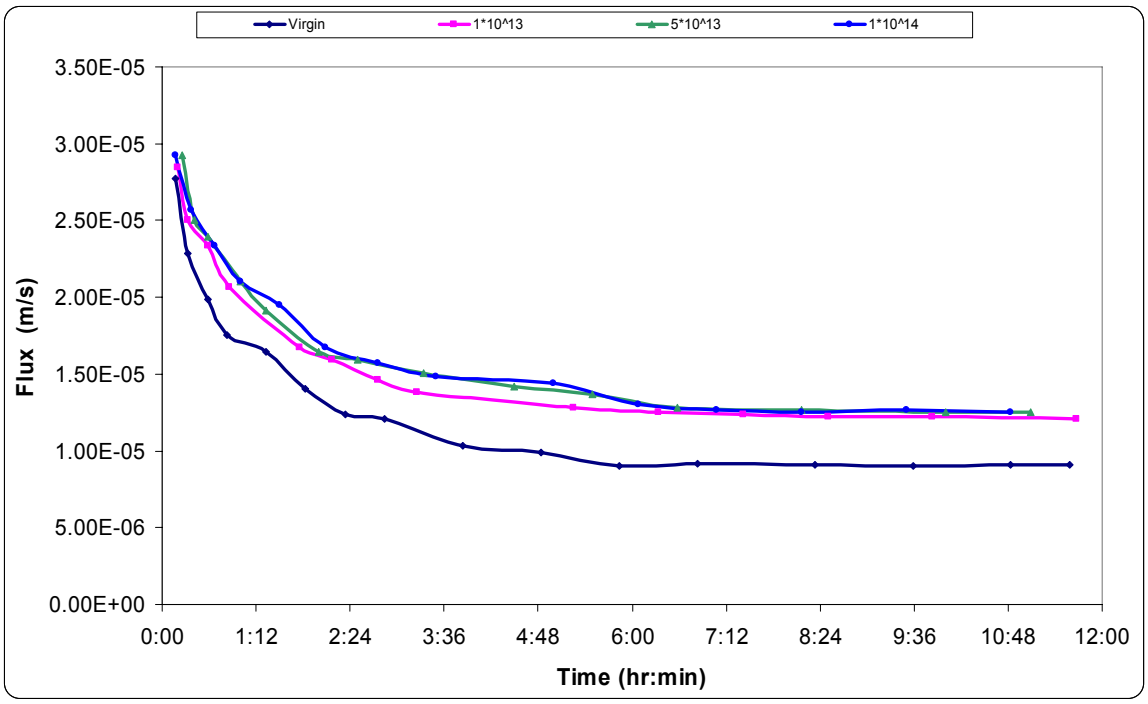


**Figure 12: Flux Vs time of virgin and irradiated membranes**

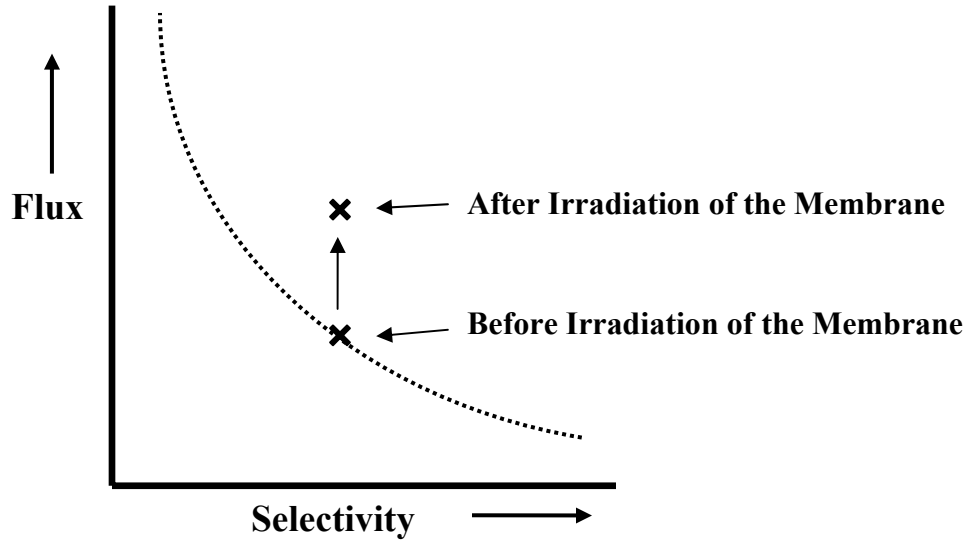


**Figure 13: Relationship between Flux and Selectivity**

Fig.14 shows AFM analyses for the virgin and irradiated membranes, after approximately 12 hours of testing. The analyses show that the average roughness of the virgin membrane was approximately 104.34 nm (±7.46 nm), while those of irradiated membranes with ion fluences of $1\times10^{13}$ ions/cm$^2$, $5\times10^{13}$ ions/cm$^2$, and $1\times10^{14}$ ions/cm$^2$ were 91.34 nm (± 5.42 nm), 87.41 nm, (±5.22 nm) and 86.96 nm (±6.86 nm) respectively. The decreases in

roughness were 12.5%, 16.2%, and 16.7% after irradiation with ion fluences of $1\times10^{13}$ ions/cm$^2$, $5\times10^{13}$ ions/cm$^2$, and $1\times10^{14}$ ions/cm$^2$, respectively, from the virgin membrane. The trend of decrease in roughness with ion fluence is shown in fig.15. The analyses indicates that cake accumulation on the virgin membrane occurred faster than and was significantly greater than on the irradiated membranes.

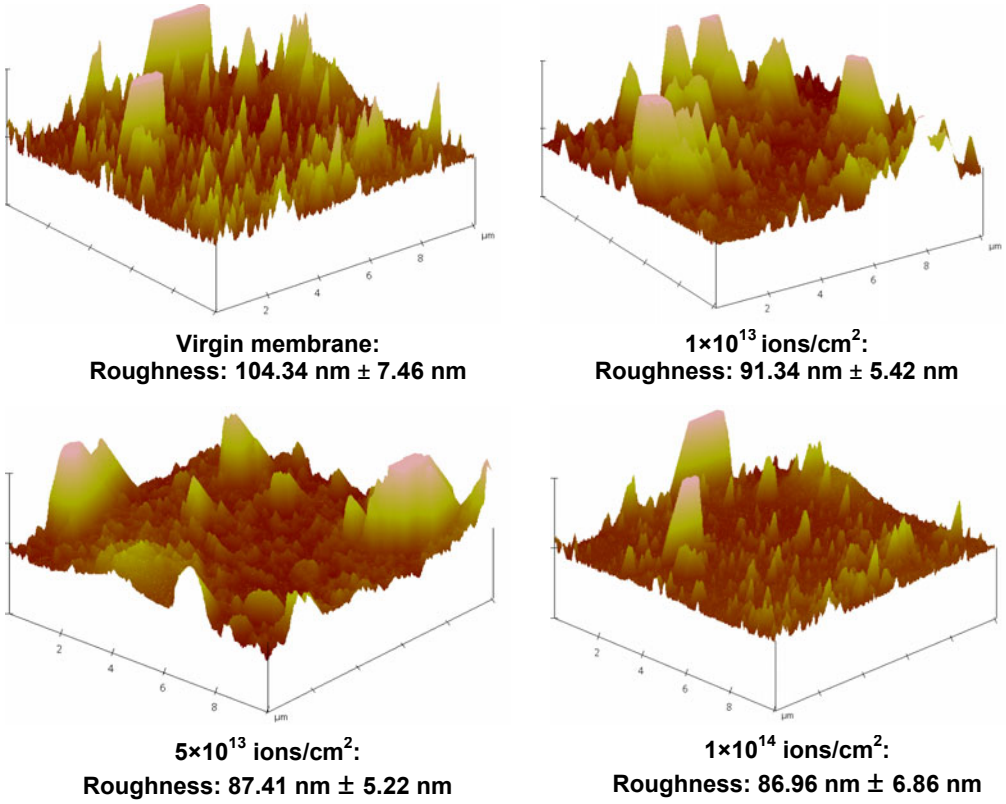


**Figure 14: AFM analysis of the virgin and irradiated membranes after filtration**

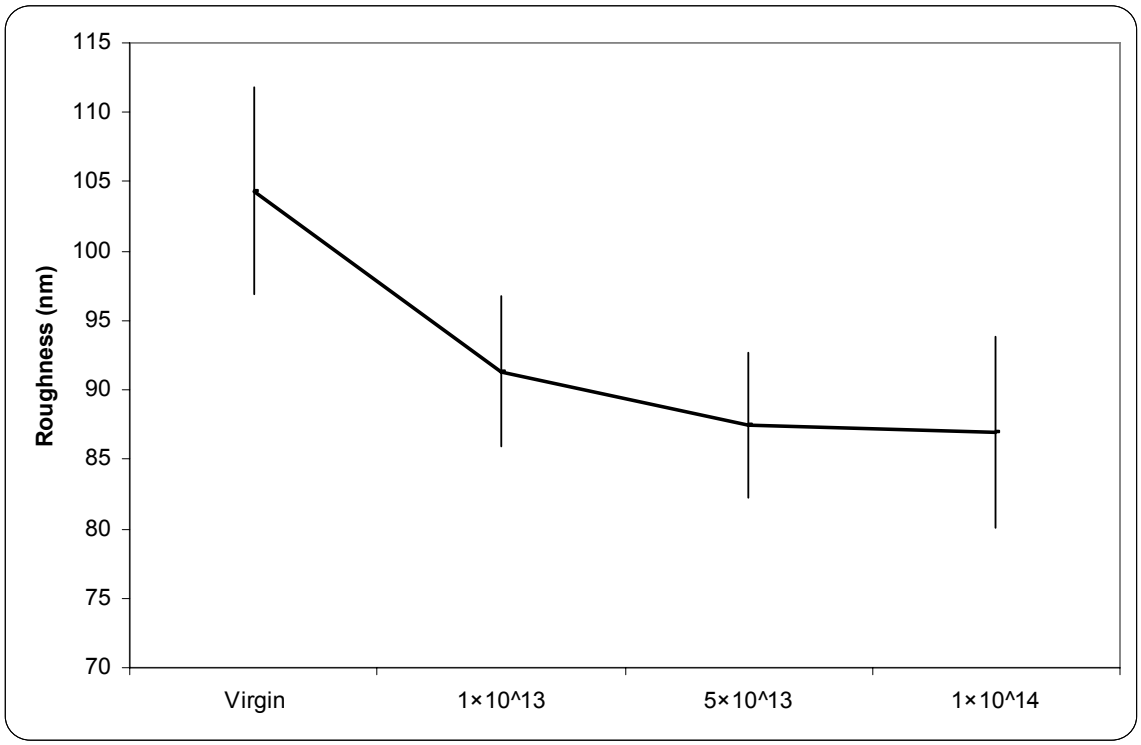


**Figure 15: Roughness of the virgin and the irradiated membranes after filtration**

Surface roughness is an important characteristic of the membrane, which influences the rate and extent of fouling [15, 16]. A membrane that exhibits high roughness inherently has distinct peaks and valleys. The valleys provide paths of least resistance, therefore a majority of permeate is transported through the membrane via these valleys. However, during operation, the valleys easily become clogged, which initiates membrane fouling and leads to flux decline and eventually complete blockage of the membrane pores. Therefore, the decrease in roughness of the membrane after ion beam irradiation resulted in decrease in fouling of membrane and an increase in flux of the membrane.

## Conclusions

The major impacts of ion beam irradiation as a post-synthesis modification technique were that:

- Ion beam irradiation resulted in rearrangement of atoms in the membrane, microstructure alterations of the surface layer, and decrease in roughness.
- The decrease in roughness of the membrane after ion beam irradiation resulted in decrease in fouling and an increase in flux of the membrane.
- Hydrophobic character and pore size distribution of the membrane were not changed after ion beam irradiation.
- The separation capabilities of the membrane were not affected after ion beam irradiation.
- Ion beam irradiation resulted in an increase in flux without changing the selectivity of the membrane; therefore the characteristic inverse relationship between flux and selectivity was improved.

- Since the improvement of the membrane properties among the various ion fluences is very less, it is better to operate at low ion fluence of $1\times10^{13}$ ions/cm$^2$, as the time taken to irradiate at this fluence is very small when compared to other fluences.

**Acknowledgments:**

This project was funded by the National Science Foundation grant CTS 03-31778. The authors acknowledge Dr. Peter Simpson (University of Western Ontario) and Dr. Victor H. Rotberg (University of Michigan) where irradiation was performed and Dr. Mark Wilk for providing membrane samples.

**References**

[1] Escobar IC, Hoek EM, Gabelich CJ, DiGiano FA, Le Gouellec YA, Berube P, Howe KJ, Allen J, Atai KZ, Benjamin MM, Brandhuber PJ, Brant J, Chang YJ, Chapman M, Childress A, Conlon WJ, Cooke TH, Crossley IA, Crozes GF, Huck PM, Kommineni SN, Jacangelo JG, Kaeimi AA, Kim JH, Lawler DF, Li QL, Schiddeman LC, Sethi S, Tobiason JE, Tseng T, Veerapanemi S, Zander AK. Recent advances and research needs in membrane fouling. *Journal American Water Works Association* 97 (2005) 79-89.

[2] J. Davenas, X.L. Xu, G. Boiteux, and D. Sage. Relation between structure and electronic properties of ion irradiation polymers. *Ncl. Instr. and Meths*. in Phys. Res.8&9 (1989) 754-763.

[3] X.L. Xu, J.Y. Dolveck, G. Boiteux, M. Escoubes, M. Monchanin, J.P. Dupin, and J. Davenas. A new approach to microporous materials – application of ion beam technology to polyimide membranes. *Mat. Res. Soc. Symp. Proc.* 354 (1995a) 351-356.

[4] X.L. Xu, J.Y. Dolveck, G. Boiteux, M. Escoubes, M. Monchanin, J.P. Dupin, and J. Davenas. Ion beam irradiation effect on gas permeatin properties of polyimid films. *Journal of Applied Polymer Science* 55 (1995b) 99-107.

[5] X.L. Xu, and M.R. Coleman. Atomic force microscopy images of ion-implanted 6FDA-pMDA polyimide films. *Journal of Applied Polymer Science* 66 (1997) 459-469.

[6] E.H. Lee. Ion-beam modification of polymeric materials: Fundamental principles and applications. *Nuclear Instruments and Methods in Physics Research B* 151 (1999) 29-41.

[7] X. Xu and M.R. Coleman. Ion beam irradiation: An efficient method to modify the sub-nanometer scale microstructure of polymers in a controlled way. *Mat. Res.Soc. Symp. Proc.,* 540 (1999a) 255-260.

[8] X. Xu and M.R. Coleman. Preliminary investigation of gas transport mechanism in a $H^+$ irradiated polyamide-ceramic composite membrane. *Nuclear Instruments and methods in Physics Research b.,* 152 (1999b) 325-334.

[9] X.L. Xu, M.R. Coleman, U. Myler, and P.J. Simpson. Post-synthesis method for development of membranes using ion beam irradiation of polimide thin films. In I. Pinnau & B.D. Freeman (Eds.), *Membrane Formation and Modification (*pp. 205-227*).* Washington, D.C.: Oxford University Press, 2000.

[10] M. Mänttäri, L. Puro, J. Nuortila-Jokinen, and M. Nyström. Fouling effect of polysaccharides and humic acid in nanofiltration. *Journal of Membrane Science* 165 (2000) 1-17.

[11] J.F. Ziegler, J.P. Biersack, and U. Littmark, U. (Eds.). *The stopping and range of ions in solids, Volume 1*. New York: Pergamon Press, 1985.
[12] M. Khayet, T. Matsuura. Determination of surface and bulk pore sizes of flat-sheet and hollow-fiber membranes by atomic force microscopy, gas permeation and solute transport methods. *Desalination* 158 (2003) 57-64.

[13] S. Hong, and M. Elimelech. Chemical and Physical Aspects of Natural Organic Carbon (NOM) Fouling of Nanofiltration Membranes. *Journal of Membrane Science* 132 (1997) 159-181.
[14] G. Socrates. Infrared Characteristic Group Frequencies, John and Wiley & Sons, 1980.
[15] W.R. Bowen and T.A. Doneva. Atomic Force Microscopy Studies of Membranes: Effect of Surface Roughness on Double-Layer Interactions and Particle Adhesion. *Journal of Colloid and Interface Science* 229 (2000) 544.
[16] E.M. Vrijenhoek, S. Hong, and M. Elimelech. Influence of membrane surface properties on initial rate of colloidal fouling of reverse osmosis and nanofiltration membranes. *Journal of Membrane Science* 188 (2001) 115-128.